SAND2017-12662C

Modeling PMDI-based Polyurethane Foam Decomposition in Pressurizing Systems Using Porous Flow and Vapor-Liquid Equilibrium

Sarah N. Scott[a,b,*], Ryan M. Keedy[a], Victor E. Brunini[a], Matthew W. Kury[a], Amanda B. Dodd[a], James L. Urban[b], A. Carols Fernandez-Pello[b]

[a] *Sandia National Laboratories, 7011 East Avenue, Livermore 94551, USA*
[b] *University of California Berkeley, Department of Mechanical Engineering, Berkeley 94720, USA*

Abstract

Polymer foam encapsulants provide mechanical, electrical, and thermal isolation in engineered systems. In fire environments, gas pressure from thermal decomposition of polymers can cause mechanical failure of sealed systems. To investigate the heat transfer and the pressurization of such systems, a 2-D finite element conduction-radiation model with porous media flow and a decomposition chemistry model was created. The gas velocity is solved by applying the Darcy approximation, and the heat transfer and pressurization are determined by solving the continuity, species, and enthalpy equations in the condensed and gas phases. Experiments show that the rate of pressurization and the local temperatures are dependent on orientation with respect to gravity, indicating buoyancy-driven flow. In addition, at the high temperatures and pressures seen in these experiments, it is expected that the organic decomposition products will exist in both the liquid and gaseous phases. In this work, a vapor-liquid equilibrium (VLE) model was added to determine the phase of the decomposition products. Models with and without the VLE effects are compared to experiment. Adding the VLE model improved agreement with experiment, and removed the need for some calibration. Uncertainty of the model including VLE effects is quantified using a Latin Hypercube approach, and sensitivities are ranked using the Pearson correlation. Results show that the parameters the model is most sensitive to depends on the response, but generally, the density of the steel, the density of the foam, and the pyrolysis reactions are major drivers of the response.

Keywords: porous media flow, polyurethane, fire, heat transfer, vapor-liquid equilibrium

1. Introduction

Polymers and other organic materials have a long history of use in engineered systems to provide mechanical, electrical, and thermal isolation. These polymers create gases when they thermally decompose, and when placed in a hermetically sealed system, they can cause a violent breach. Accurately modeling organic materials in high heat environments is therefore crucial for systems safety analysis, but challenging due to complex physics, uncertain thermal properties, and the relatively low decomposition temperatures. When polymers are exposed to a source of heat, such as fire, they undergo both physical and chemical changes [1]. The chemical breakdown, or decomposition, of the polymer causes large molecules to fragment, forming a variety of smaller molecules that can pressurize a system, cause new heat transfer paths, and take on new material properties.

Polymer foams have been studied for many years due to their wide use in residential applications [2] as well as engineered systems. To successfully model the ignition of polyurethane, a chemical kinetics mechanism that controls pyrolysis must be proposed. This is typically done by performing thermogravimetric analysis combined with Fourier transform infrared spectroscopy (TGA-FTIR) [3, 4]. To successfully simulate the pyrolysis of a solid, more than just the kinetic mechanism must be modeled. Heat, momentum, and mass transfer must also be considered. These simulations have been performed for a variety of materials, from woods and other natural materials [5], to polymers such as PMMA [6], and polyurethanes [7]. Darcys law has been used to numerically study the flame stabilization in a porous burner [8, 9], as well as the flow through a pyrolyz-

*Corresponding author:
Email address: snscott@sandia.gov (Sarah N. Scott)

ing medium [10, 11]. Darcys law has also been used to study the heat and mass transport in developing char layers in polymers [12].

The liquid phase is also of interest when studying pyrolyzing polymers. For thermoplastics, an external heat source can cause the polymer to melt and flow. Melting polymers can change the flammability properties of the material [13] as well affect the upward flame spread [14]. The melting of the polymers can also cause the dripping and pooling of flammable liquid [15, 16].

One challenge with developing numerical models is determining the material and chemical properties of the materials being modeled. Optimization methods, such as genetic algorithms, shuffled complex evolution, and sequential quadratic programming can be useful in this regard [17–20]. Statistics can be brought to bear not only on model calibration but also model uncertainty [21, 22] and sensitivity [23, 24]. These methods can also be combined to conduct rigorous validation of a model [25, 26], or to understand the probability of an event occurring, for example, power cable failure [27]. While these are all powerful tools, it has been shown that once uncertainty is propagated through a high number of reaction mechanisms, the resulting spread in the simulated data can be larger than when using a smaller number of mechanisms [28, 29].

This work presents a porous media plus Arrhenius-rate based chemistry modeling technique used to describe the decomposition, heat transfer, and pressurization of polymeric methylene diisocyanate (PMDI)-polyether-polyol-based polyurethane foam when heated in a sealed container. A vapor-liquid equilibrium (VLE) model was added, as at the temperature and pressures seen within the can, it is possible for the decomposition products to be in the condensed or vapor phase. The results of the new model (PM-VLE) are compared with experiment, as well as with the previous porous media only (PM-O) model. Uncertainty for the PM-VLE model is quantified, and sensitivities are discussed.

2. Experimental Motivation

Prior experimental work studied PMDI decomposition in a configuration consisting of a cylindrical stainless steel container filled with foam along with an embedded metal object (Fig. 1). Experiments were performed in upright and inverted orientations (Fig. 2), and pressure and temperature were monitored. The lid was maintained at that temperature until the gases generated by the decomposing foam caused the can to breach. A summary of these experiments can be found in [30]. The inverted experiments are shorter in duration than the upright experiments, due to faster pressurization. This difference in response is believed to be caused by the flow of both liquid and gaseous decomposition products.

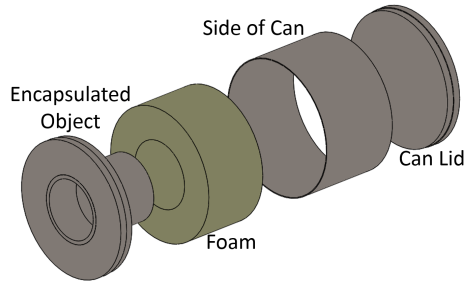

Figure 1: Exploded view of the geometry

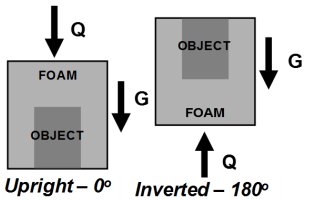

Figure 2: Description of upright and inverted heating, where Q is the externally applied heat flux and G is gravity

3. Computational Model

3.1. Porous Media

The porous media model approach assumes the can is filled with foam that may exist in two phases: the condensed (solid) phase and the gas phase. The condenced phase foam has an associated porosity, which is a function of reaction. In the gas phase, Darcy's law is used to approximate the flow of the fluid and the continuity, species, and enthalpy conservation equations are solved. The ideal gas equation of state is used to relate pressure and density. In the condensed phase, the species and enthalpy equations are solved, and the two phases are coupled through source terms in the species equations and a volumetric heat transfer term in the enthalpy equations. This derivation is based on the model in Lautenberger *et al.* [31].

In this model, the conductivities of the char and virgin foams are determined by summing the volume averaged conductivities for each solid phase. An effective radiative conductivity is then added to this value, based on the diffuse approximation for radiation heat transfer

Table 1: Major decomposition products

Molecule	Formula	Molar Mass (g/mol)
Propylene glycol	$C_3H_8O_2$	76
Aniline	$C_6H_5NH_2$	93
4-methylaniline	C_7H_9N	107
Phenyl isocynatate	C_7H_5NO	119

through an optically thick medium. The reaction kinetics were derived through TGA-FTIR [32–34], and approximated by:

$$FOAMA \rightarrow 0.56CO_2 + 0.44LMWO \quad (1a)$$

$$FOAMB \rightarrow HMWO \quad (1b)$$

$$FOAMC \rightarrow 0.5char + 0.5HMWO \quad (1c)$$

Where $FOAMA$, $FOAMB$, and $FOAMC$ are representative moieties of PMDI, comprising fractions of 0.45, 0.15 and 0.4, respectively. Low molecular weight organics ($LMWO$) and high molecular weight organics ($HMWO$) represent two general classes of organic molecules with an average weight of 80 and 120 g/mol, respectively. Table 1 shows a list of the major decomposition products detected through FTIR. The organic products listed in Table 1 have saturation pressures such that they are expected to condense at the pressures and temperatures seen experimentally. With this in mind, the amount of the organics that go into the gas versus condensed phase was among the four parameters that were calibrated for the PM-O model. The other three were: the permeabilities of the virgin and char foams, and the Rosseland-mean extinction coefficient for the char that appears in the effective conductivity for radiative heat transfer [35]. The results of this study indicated the importance of the having a physics based method for determining the gas/condensed split.

3.2. Vapor-Liquid Equilibrium

To this end, vapor-liquid equilibrium equations were added to the porous media framework. For each species participating in the vapor-liquid equilibrium (CO_2, HMWO, LMWO) a reaction representing the evaporation and condensation of the species is incorporated in the model:

$$CO_2^{\text{liquid}} \leftrightarrow CO_2^{\text{gas}}$$

$$HMWO^{\text{liquid}} \leftrightarrow HMWO^{\text{gas}}$$

$$LMWO^{\text{liquid}} \leftrightarrow LMWO^{\text{gas}}$$

The rate of each of these reactions is modeled using a form of the Hertz-Knudsen equation [36], modified to allow for non-ideal behavior by using the fugacity of the species in each phase in place of the pressure and saturation pressure:

$$\omega = \frac{A}{2 - C_c}\sqrt{\frac{2}{\pi MRT}}(C_e f_{\text{liquid}} - C_c f_{\text{gas}}) \quad (3)$$

where A is the specific surface area, M the molecular weight of the species, C_e and C_c the evaporation and condensation coefficients, and f_{liquid} and f_{gas} the fugacities of the species in each phase respectively. For the purposes of the VLE model we are primarily interested in modeling equilibrium and have no data on the kinetics of the phase change. In these mixtures $C_e = C_c$ and is sufficiently large to maintain equilibrium but not make the kinetics unnecessarily stiff. Each gas-phase species are treated as ideal, so $f_{\text{gas}} = P_i$ where P_i is the partial pressure of the species. The fugacities of the HMWO and LMWO liquid species are modeled using the Antoine equation:

$$\log_{10}\left(f_{\text{liquid}}\right) = A - \frac{B}{T + C} \quad (4)$$

with coefficients based on aniline. Finally, the fugacity of CO_2 in the liquid phase is modeled using Henry's law $f_{\text{liquid}} = H(T)$ since there is interest in regimes above the critical pressure of CO_2.

For both the PM-VLE and PM-O models, a 2-D finite element model composed of tetrahedral elements was evaluated in the Sierra Thermal/Fluids multiphysics code [37] to computationally simulate the experiments. Convective and radiative boundary conditions were applied to all sides of the can, with the exception of the heated surface, where a radiative boundary condition is prescribed. The PM-VLE model used the permeabilities of the virgin and char foams and the Rosseland-mean extinction coefficient that had been optimized for the PM-O model; the calibrated constant that determined the ratio of the organics that go into the gas versus condensed phase was replaced by the VLE model.

3.3. Model Uncertainty

Model uncertainty and sensitivity were evaluated for the PM-VLE model in Dakota [38] using a Latin Hypercube Sampling (LHS) approach. See Saltelli *et al.* [39] and Helton [40] for a description of the LHS method. The LHS method requires specifying a distribution for each parameter. Because data are not available to formulate a distribution, a functional form is assumed. As a first estimate, a truncated normal distribution for each parameter (Table 2) is assumed with a mean and standard deviation. The mean is assumed to be a value of

Table 2: Parameters used in LHS method

Foam (virgin, liquid, char)	Bulk Density
	Solid Density
	Rosseland Coefficient
	Bulk Conductivity
	Specific Heat Capacity
	Permeability
	Molecular Weight
Reactions	Heat of Reaction
	Activation Energy
	Mass Fractions
Gas Products	Specific Heat Capacity
	Mass Diffusivity
	Viscosity
	Molecular Weight
	Saturation Pressure
Steel	Density
	Thermal Conductivity
	Specific Heat
	Emissivity
Boundary Conditions	Convection Coefficient
	Lid Temperature

1 that is multiplied by the nominal parameter values (*e.g.*, thermal conductivity, $k(T) = p_i k_{nom}(T)$). 420 LHS samples were selected. The parameters were varied by ±10%, except for the lid temperature (±2%), the activation energy (±2%), and the virgin foam density (±5%). The lid temperature and foam density were both reduced because they are well known, and the activation energy was reduced such that it would encompass the experimental TGA data.

When a LHS approach is used, correlation coefficients can be directly calculated provided that $n_{LHS} \geq n_p$. The correlation coefficients are computed using the following equation:

$$r = \frac{\sum_i^{n_{LHS}} (p_i - \overline{p})(R_i - \overline{R})}{(n_{LHS}\sigma_R\sigma_p)} \tag{5}$$

where n_{LHS} is the number of samples, n_p is the number of parameters, R_i is the value of the response of interest for the i^{th} simulation, $\overline{R}$ is the mean value of the response, p_i is the value for the i^{th} parameter, $\overline{p}$ is the mean value of the input parameter, σ_R is the standard deviation of the mean value of the response, and σ_p is the standard deviation of the mean value of the parameter. This approach assumes a linear correlation between the response and the parameter and is also referred to as the Pearson correlation coefficient.

4. Results and Discussion

Figure 3 compares the nominal PM-O and PM-VLE pressure responses to the experimental results with a virgin foam density of approximately 320 kg/m^3 (20 lb/ft^3) heated to 1073 K at a rate of 150 K/min. The PM-O response agrees very well with inverted experimental results. The upright results, while quantitatively similar by 900 seconds, are not in good qualitative agreement with experiment. It is important to recall that the PM-O results were calibrated to match this experimental data. Though the responses were normalized in an attempt to have them both considered to the same degree, the inverted pressure was still favored over the upright pressures and temperatures in the optimization, because its normalized values tended to increase drastically. The PM-VLE (which was not further optimized), is not as good of a quantitative result, however, the qualitative comparison, particularly for upright, is much improved. For upright, a dynamic ratio of gas to condensed organics improves the fit because, due to the of lack buoyant flow, there is a large temperature differential early in time, which allows for the condensation of liquid, and thus a lower pressure. Later in time, as the foam decomposes and the heat reaches the cooler areas of the can, the liquid evaporates, increasing the pressure again. Since the PM-O model uses a constant ratio it over-, then under-predicts, highlighting the issue.

Figure 4 compares the nominal PM-O and PM-VLE embedded object temperature response to the experimental results. As previously mentioned, though PM-O was optimized, the inverted pressure drove the optimization, thus the quantitative temperature comparison was never excellent, though it was qualitatively similar. However, the PM-VLE is both a good qualitative and quantitative match. This appears to be due to the organic vapors condensing on the (comparatively cool) encapsulated object and thus heating it faster.

To quantify the uncertainty of the PM-VLE model, the average and standard deviation of the responses from the ensemble of runs was calculated. The average result for pressure, with ±2 standard deviations for both the simulation and experimental error, is presented in Figure 5. The range of the uncertainty at the end of the simulation is 3.3 MPa for upright and 4.8 MPa for inverted. The main contributors to the uncertainty are shown in 3, in order of importance based on a response weighted time integration of Eq. 5. In general, the pressure was most sensitive to parameters that controlled the CO_2 production. This result highlights how sensitive the pressure is to the reactions. The reactions are known to be dependent on pressure, as seen in the dif-

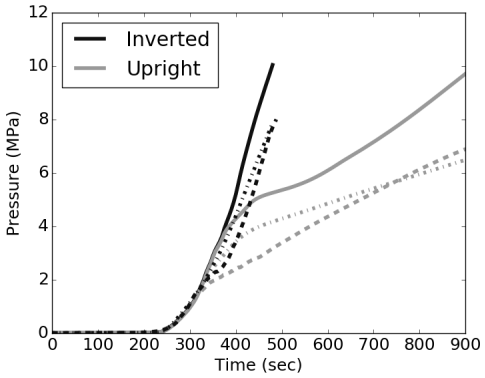

Figure 3: Nominal simulation results for the PM-VLE (solid) and PM-O (dot-dash) with experimental values (dashed) for upright (grey) and inverted (black) for the pressure in the can.

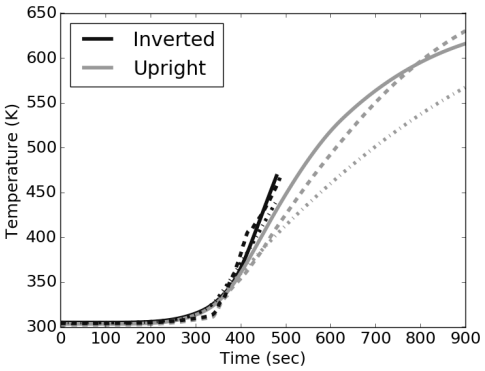

Figure 4: Nominal simulation results for the PM-VLE (solid) and PM-O (dot-dash) with experimental values (dashed) for upright (grey) and inverted (black) for the temperature of the embedded object.

Table 3: Top Five Sensitivity Results

	Inverted	**Upright**
Pressure	*FoamA* Mass Fraction	*FoamA* Mass Fraction
	Heat Flux	CO_2 Mass Fraction
	CO_2 Mass Fraction	Steel Density
	Activation Energy	Virgin Foam Bulk Density
	Virgin Foam Bulk Density	Heat Flux
Temperature	Heat Flux	Steel Density
	Steel Density	Heat Flux
	Activation Energy	Virgin Foam Bulk Conductivity
	Char Rosseland Coefficient	Activation Energy
	Foam Specific Heat	Char Rosseland Coefficien

ference between the unconfined and partially confined TGA results. Therefore, at these pressures, how much confidence is there in the reactions? These results would indicate that time spent investigating the pressure dependency of the decomposition reactions would be of high value.

The average result for the temperature of the embedded object, also with ±2 standard deviations for both the simulation and experimental error, is presented in Figure 6. The range of the uncertainty at the end of the simulation is 40 K for upright and 60 K for inverted. As seen in table 3, heat flux and steel density dominate, as is expected since the object is steel, however, the foam properties and reaction mechanisms are in play, as the most direct heat path is through the foam.

5. Conclusions

Two models to simulate thermally decomposing PMDI polyurethane foam in a pressurizing sealed system were evaluated. The PM-O model includes the necessary physics for being able to simulate orientation-dependent pressure and temperature responses through the addition of a porous media model. However, several parameters had to be calibrated, as there was no way to measure them. While pressure agreed well, the temperature of the embedded object is under-predicted. The PM-VLE model eliminated the need for one of the calibrated parameters by including vapor-liquid equilibrium for the decomposition products. The results compare well in both temperature and pressure. The uncertainty was quantified for the VLE-PM model and sensitivities were assessed using a strategy where the uncertainty in the input parameters is (mostly) equal across the parameter space. This is not necessarily reflective of reality, as there were well-known parameters, such as the heat flux, that appeared in the top five most important parameters, and unknowns, like the char permeability, that did not. However, this study is still useful for extrapolation to less well defined systems, as it serves as a guide for which parameters require the most attention.

In the future, additional heating rates should be examined, as well as a new calibration of the permeabilities and Rosseland mean extinction coefficient for the char for the PM-VLE model, to see if they differ from those found in the PM-O. Finally, now that a liquid phase can be generated, a model to advect that liquid needs to be implemented.

Acknowledgments

Sandia National Laboratories is a multimission laboratory managed and operated by National Technology and Engineering Solutions of Sandia, LLC., a wholly owned subsidiary of Honeywell International, Inc., for the U.S. Department of Energys National Nuclear Security Administration under contract DE-NA0003525. SAND2017-xxxx

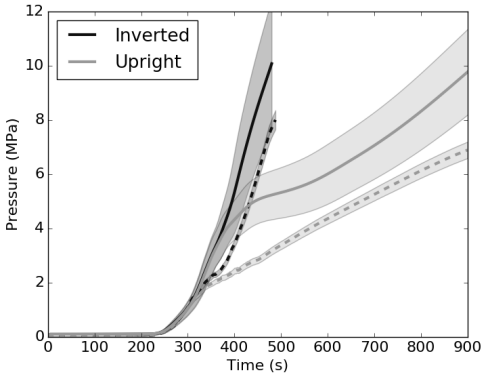

Figure 5: Simulation results (solid) with experimental values (dashed) for upright (grey) and inverted (black) for the pressure in the can. Simulation and experiment are both presented with ±2 standard deviations of the data.

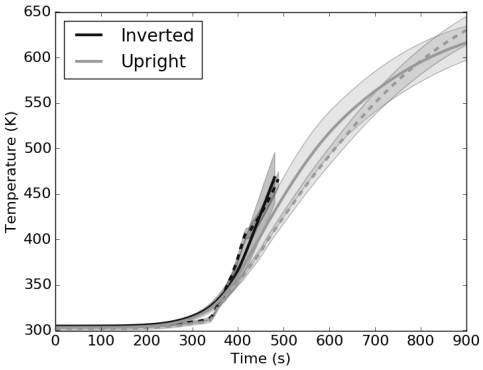

Figure 6: Simulation results (solid) with experimental values (dashed) for upright (grey) and inverted (black) for the temperature of the embedded object. Simulation and experiment are both presented with ±2 standard deviations of the data.

References

[1] C. Beyler, M. Hirschler, Thermal Decomposition of Polymers, in: SFPE Handbook of Fire Protection Engineering, National Fire Protection Association, 2001, pp. 110–131.

[2] R. Hadden, A. Alkatib, G. Rein, J. L. Torero, Radiant Ignition of Polyurethane Foam: The Effect of Sample Size, Fire Technology 50 (3) (2014) 673–691.

[3] T. Rogaume, L. B. Valencia, E. Guillaume, F. Richard, J. Luche, G. Rein, J. L. Torero, Development of the Thermal Decomposition Mechanism of Polyether Polyurethane Foam Using Both Condensed and Gas-Phase Release Data, Combustion Science and Technology 183 (7) (2011) 627–644.

[4] L. Bustamante Valencia, T. Rogaume, E. Guillaume, G. Rein, J. L. Torero, Analysis of principal gas products during combustion of polyether polyurethane foam at different irradiance levels, Fire Safety Journal 44 (7) (2009) 933–940.

[5] C. D. Blasi, Analysis of Convection and Secondary Reaction Effects Within Porous Solid Fuels Undergoing Pyrolysis, Combustion Science and Technology 90 (5) (1993) 315–340.

[6] I. Vermesi, N. Roenner, P. Pironi, R. M. Hadden, G. Rein, Pyrolysis and ignition of a polymer by transient irradiation, Combustion and Flame 163 (2016) 31–41.

[7] O. M. Putzeys, A. C. Fernandez-Pello, G. Rein, D. L. Urban, The piloted transition to flaming in smoldering fire retarded and non-fire retarded polyurethane foam, Fire and Materials 32 (8) (2008) 485–499.

[8] A. J. Barra, J. L. Ellzey, Heat recirculation and heat transfer in porous burners, Combustion and Flame 137 (1-2) (2004) 230–241.

[9] A. J. Barra, G. Diepvens, J. L. Ellzey, M. R. Henneke, Numerical study of the effects of material properties on flame stabilization in a porous burner, Combustion and Flame 134 (4) (2003) 369–379.

[10] A. Dodd, C. Lautenberger, A. Fernandez-Pello, Numerical examination of two-dimensional smolder structure in polyurethane foam, Proceedings of the Combustion Institute 32 (2) (2009) 2497–2504.

[11] A. B. Dodd, C. Lautenberger, C. Fernandez-Pello, Computational modeling of smolder combustion and spontaneous transition to flaming, Combustion and Flame 159 (1) (2012) 448–461.

[12] J. Staggs, Heat and mass transport in developing chars, Polymer Degradation and Stability 82 (2) (2003) 297–307.

[13] C. Denecker, J. J. Liggat, C. E. Snape, Relationship between the thermal degradation chemistry and flammability of commercial flexible polyurethane foams, Journal of Applied Polymer Science 100 (4) (2006) 3024–3033.

[14] J. Zhang, T. Shields, G. Silcock, Effect of melting behaviour on flame spread of thermoplastics, Fire and Materials 21 (1).

[15] K. M. Butler, A model of melting and dripping thermoplastic objects in fire, Fire and materials (2009) 341–352.

[16] K. M. Butler, E. Oate, S. R. Idelsohn, R. Rossi, Modeling polymer melt flow using the particle finite element method, in: Eleventh International Interflam Conference, London, England, 2007, pp. 929–940.

[17] G. Rein, C. Lautenberger, A. Fernandez-Pello, J. Torero, D. Urban, Application of genetic algorithms and thermogravimetry to determine the kinetics of polyurethane foam in smoldering combustion, Combustion and Flame 146 (1-2) (2006) 95–108.

[18] M. Bruns, J. Koo, O. Ezekoye, Population-based models of thermoplastic degradation: Using optimization to determine model parameters, Polymer Degradation and Stability 94 (6) (2009) 1013–1022.

[19] S. Garcia, J. Guynn, E. P. Scott, Use of Genetic Algorithms In Thermal Property Estimation: Part Ii - Simultaneous Estimation Of Thermal Properties, Numerical Heat Transfer, Part A: Applications 33 (2) (1998) 149–168.

[20] M. Chaos, M. M. Khan, N. Krishnamoorthy, J. L. de Ris, S. B. Dorofeev, Evaluation of optimization schemes and determination of solid fuel properties for CFD fire models using bench-scale pyrolysis tests, Proceedings of the Combustion Institute 33 (2) (2011) 2599–2606.

[21] K. J. Overholt, O. A. Ezekoye, Quantitative testing of fire scenario hypotheses: a bayesian inference approach, Fire Technology 51 (2) (2015) 335–367.

[22] M. C. Bruns, Inferring and Propagating Kinetic Parameter Uncertainty for Condensed Phase Burning Models, Fire Technology 52 (1) (2016) 93–120.

[23] S. I. Stoliarov, N. Safronava, R. E. Lyon, The effect of variation in polymer properties on the rate of burning, Fire and Materials 33 (6) (2009) 257–271.

[24] G. T. Linteris, Numerical simulations of polymer pyrolysis rate: Effect of property variations, Fire and Materials 35 (7) (2011) 463–480.

[25] P. Summers, B. Lattimer, S. Case, S. Feih, Predicting compression failure of composite laminates in fire, Composites Part A:

Applied Science and Manufacturing 43 (5) (2012) 773–782.
[26] P. Summers, B. Lattimer, S. Case, S. Feih, Sensitivity of thermo-structural model for composite laminates in fire, Composites Part A: Applied Science and Manufacturing 43 (5) (2012) 783–792.
[27] A. Matala, S. Hostikka, Probabilistic simulations of cable fires in a cable tunnel, in: 20th international conference on structural mechanics in reactor technology, Helsinki, Finland, 2009.
[28] N. Bal, G. Rein, On the effect of inverse modelling and compensation effects in computational pyrolysis for fire scenarios, Fire Safety Journal 72 (2015) 68–76.
[29] N. Bal, G. Rein, Relevant model complexity for non-charring polymer pyrolysis, Fire Safety Journal 61 (2013) 36–44.
[30] S. N. Scott, A. B. Dodd, M. E. Larsen, J. M. Suo-Anttila, K. L. Erickson, Validation of heat transfer, thermal decomposition, and container pressurization of polyurethane foam using mean value and latin hypercube sampling approaches, Fire Technology 52 (1) (2016) 121–147.
[31] C. Lautenberger, C. Fernandez-Pello, Generalized pyrolysis model for combustible solids, Fire Safety Journal 44 (6) (2009) 819–839.
[32] K. Erickson, A. Dodd, R. Hogan, K. J. Dowding, Heat Transfer, Foam Decomposition, and Container Pressurization: Comparison of Experimental and Modeling Results, Interscience Communications Ltd, Nottingham, UK, 2010.
[33] K. L. Erickson, A. Dodd, E. Quintana, Physical Behavior and Container Pressurization During Thermal Decomposition of Polyurethane Foams, in: Proceedings of BCC 2011, Stamford, 2011.
[34] K. L. Erickson, Thermal decomposition mechanisms common to polyurethane, epoxy, poly (diallyl phthalate), polycarbonate and poly (phenylene sulfide), Journal of Thermal Analysis and Calorimetry 89 (2) (2007) 427–440.
[35] S. N. Scott, R. M. Keedy, V. E. Brunini, A. B. Dodd, Modeling Porous PMDI-based Polyurethane Foam Decomposition in Pressurizing Systems, College Park, Maryland, 2017.
[36] M. Knudsen, The kinetic theory of gases: some modern aspects.
[37] Sierra Core Team, Sierra Thermal Fluids Code (2017).
[38] B. Adams, L. Bauman, W. Bohnhoff, K. Dalbey, M. Ebeida, J. Eddy, M. Eldred, P. Hough, K. Hu, J. Jakeman, J. Stephens, L. Swiler, D. Vigil, T. Wildey, Dakota, A Multilevel Parallel Object-Oriented Framework for Design Optimization, Parameter Estimation, Uncertainty Quantification, and Sensitivity Analysis: Version 6.0 Users Manual, SAND2014-4633 (Jul. 2014).
[39] A. Saltelli, K. Chan, E. Scott, Chapter 6, in: Sensitivity analysis, Wiley, New York.
[40] J. Helton, Latin hypercube sampling and the propagation of uncertainty in analyses of complex systems, Tech. Rep. SAND2001-0417, Sandia National Laboratories, Albuquerque (2001).